COLE-NL-72-1212

Electrical measurements in silicon under shock-wave compression*

N. L. Coleburn, J. W. Forbes, and H. D. Jones
Naval Ordnance Laboratory, White Oak, Silver Spring, Maryland 20910
(Received 9 June 1972)

The electrical behavior of p-type silicon in the (111) orientation was studied under shock stresses from 8 to 160 kbar. Positive electrical signals are induced in the crystals during passage of elastic shock waves. Maximum signal amplitude was detected below the Hugoniot elastic limit (55 kbar). Resistance-vs-stress measurements were made when the polarization signal was zero, i.e., no elastic waves were in the crystals. The resistance becomes very small near the elastic limit, indicating that a metallic state is reached. The relative resistance, R/R_o, then increases significantly at 133 kbar where a phase transition is indicated.

INTRODUCTION

The major purpose of this study was to measure the electrical resistance of p-type silicon as a function of temperature and pressure under shock conditions. The data could be used to obtain the energy gap between the impurity level and the conduction band or, combined with the thermal effect on the static pressure—energy-gap data, the temperature in the shock specimen could be determined. Also, resistance measurements during planar shock loading of Si in a known crystallographic direction could give an understanding of silicon's transition states. The resistance data should provide a test of Pavlovskii's[1] interpretation of the discontinuity in his dynamic compressibility (Hugoniot) measurements. Pavlovskii interpreted the discontinuity as a metallic transition state at ~100 kbar. This value is 100 kbar lower than the static pressure transition state speculated as metallic by Minomura and Drickamer[2] from static resistance-pressure measurements. Wentorf and Kaspar,[3] using static resistance-pressure measurements also, detect transition states in silicon and cite two regions of ~thousandfold reduction in resistivity, within 110—120 kbar and 150—160 kbar.

Electrical measurements in solids during the microsecond intervals of shock compression are complicated by anisotropic compression by elastic shocks, by creation of structure defects by plastic shocks, and often by large electrical polarization signals. There have been a number of recent studies of electrical signals generated in dielectrics[4,5] and nonpiezoelectric ionic solids[6] during compression by shock waves. The existence of shock-induced polarization in doped Si was reported recently by Mineev *et al.*[7] We also reported measurements of polarization in silicon.[8] We have continued polarization measurements to explain the origin of the signals and their magnitude. The shock-resistance data of this paper also help identify the transition states of silicon.

The electrical measurements were made in silicon single crystals of (111) orientation with a p-type carrier concentration of ~10^{14} cm^{-3} and a resistivity of ~50 Ω cm. The duration of shock compression was ~1 μsec. Pressures were in the 8—160-kbar range. The polarization results indicate that only positive charges were generated during passage of the shock wave. The maximum signal amplitude occurred when the stress was below the Hugoniot elastic limit (HEL) of 55 kbar. We discuss a model of polarization based on a double charge layer across the elastic shock. The order of magnitude of the signal can be explained by such a model. The shock-resistance measurements imply that doped silicon is converted from a semiconductor to a metallic state at stresses near the HEL. The resistance, however, increases significantly at higher shock stresses. The analysis correlating the electrical measurements with the shock-compression results leads us to believe that silicon acts as an elastic-plastic solid.

EXPERIMENTAL

In the electrical and Hugoniot measurements, the crystals were oriented with their faces perpendicular to the (111) plane. Shock compression was accomplished by a plane shock wave which propagated perpendicularly to the crystal face. By explosively producing plane shock waves in systems consisting of materials of different shock impedance, a wide range of stresses was transmitted to the Si crystals. The stress pulses were essentially square steps, i.e., not changing in stress amplitude during the shock transit. Measurements of the shock waves in the crystals and the driver plate were made by light-reflection techniques described previously,[9,10] and were used to derive Hugoniot equation-of-state data for silicon. These measurements and those of Gust and Royce[11] provide the calibrated stress points that are given in this paper. Table I gives the shock driving systems used to obtain different stress amplitudes in the crystal specimens. The induced polarization signals were used to study the shock-wave structure and to establish shock-wave transit times from which shock-wave velocities were calculated.

The geometry for observing the electrical signals, Fig. 1, was similar to that of a parallel-plate capacitor with the Si crystal mounted between the electrically grounded shock driver and the aluminum back-up electrode. Since no voltage was applied in the polarization experiments, the back-up electrode was also initially at ground potential. The end faces of the crystals (2.2 cm in diameter and 0.32 cm high) were coated with a vapor-deposited aluminum layer, ~3 μ thick. To assume Ohmic contact surfaces, the coated crystals were heated in an oven for 30 min at ~550 °C. Charges generated within the p-type Si during the shock transit were measured by a recording oscilloscope as a voltage drop across a 50-Ω load resistor which shunted the back-up electrode to ground. In the resistance measurements, a voltage, usually 1.3 V negative, was applied across the crystal faces through a constant current power supply. To minimize resistance heating, the timing of the current pulse was controlled so that the pulse was imposed ~5 μsec prior to the shock-wave compression of the crystal. Silicon-controlled rectifiers were used to switch

TABLE I. Shock driving systems.

System No.	Explosive and thickness (cm)	Shock attenuator and thickness (cm)	Specimen plate and thickness (cm)	Stress[a] (kbar) Specimen plate	Silicon
1	2.54 DATB		2.54 steel	129	82
2	2.54 Pentolite	0.32 A./0.32 Plexiglas 2.54 steel	0.32 Al	87	(90)
3	2.54 Pentolite		2.54 steel	129	82
4	2.22 Nitromethane	1.27 brass/2.54 Plexiglas	0.64 Al	50	59
5	2.54 Pentolite	1.27 Al/1.27 phenolic resin	1.27 Al	130	133
6	1.27 Comp B		1.27 brass	298	162
7	2.54 DATB/Nylon	0.64 Plexiglas	0.64 Al	(177)	(162)

[a]Stresses are known to ± 10% except for values in parentheses which are known to ± 15%.

the current on when probe switches imbedded in the driver plate were contacted by the shock-wave front.

WAVE PROPAGATION

The x-t diagram, Fig. 2, gives some insight into the shock-wave structure and its effects on the electrical characteristics of silicon. The diagram describes shock propagation measurements in (111) Si crystals at a stress level of 162 kbar (e.g., system 6, Table I). The numbers in the diagram denote certain times of wave arrival or wave interactions corresponding to the events marked with the same numerals[12] in the electrical records (see Fig. 3). Stress levels identified with these events were obtained using impedance matching and a simple elastic-plastic model.

We observe that three forward-facing waves originate at the specimen-plate—Si boundary when plane shock compression of the crystal begins with stress levels behind the waves of 55, 133, and 162 kbar, respectively. At the time marked (2) in Fig. 2, the 55-kbar elastic precursor traveling at 9.6 mm/μsec in (111) Si reaches the Si—aluminum-electrode interface, and a backward-facing relief wave with a stress gradient of 9 kbar is reflected from the aluminum electrode. This wave continues backward, relieving the stress in the states behind the two advancing plastic shocks. It interacts at (3) with the first plastic shock. The state just ahead of this shock, however, is now at a stress of 46 kbar but can withstand 55 kbar (HEL). Therefore, the first plastic shock after the interaction separates into two new forward-facing shock waves, an elastic shock with a stress gradient of 9 kbar and a plastic shock. The second elastic shock arrives at the electrode at (5). Again a shock wave is transmitted to the aluminum electrode and a relief wave is reflected into the crystal but now with a stress gradient of only 1 kbar.

Similar interactions recur producing splitting of the plastic shocks as described above. However, no further relief waves are shown reflected from the aluminum-electrode—crystal boundary, since the elastic shocks now are very weak and the shock impedances of Si and Al in their elastic compression states now are essentially the same. The first plastic wave front reaches the electrode at (6) where a 10-kbar shock is reflected back into the silicon. [The stress—particle-velocity (P-u) curve of aluminum crosses and goes above the silicon P-u curve at ~115 kbar, which is the reason a shock wave is reflected at (6).] The second plastic wave reaches the electrode at (7) where an 8-kbar shock is reflected back into the silicon. The stresses behind the various waves in the crystals are all within the range 155—175 kbar for at least 0.25 μsec after time (7) if the relief from the edges can be ignored.

The above description of the shock- wave structure in (111) Si is based on optical measurements of the free-surface motion, wave transit times obtained from oscillograph records of the electrical response of the crystals to shock loading, and shock-resistance measurements. These measurements show that Si stressed to 162 kbar in the (111) direction has just two phase transitions, the elastic-plastic transition at ~55 kbar and a polymorphic transition at ~133 kbar. This result differs from the interpretation of Gust and Royce based on free-surface motion measurements. Their interpretation would have the second wave arriving at (5) in Fig. 2 be a plastic shock centered at the x-t origin and due to another polymorphic transition at ~110 kbar. Our free-surface velocity values agree with Gust and Royce's[11] values but our interpretation, supported by electrical measurements, disagrees as to the origin and type of wave arriving at (5). Both of the above interpretations of silicon's Hugoniot could explain the measured free-surface motions but Gust and Royce's

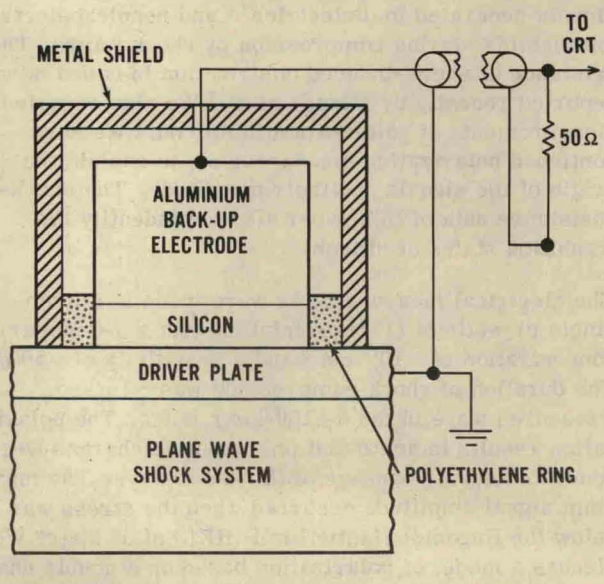

FIG. 1. Experimental arrangement for observing shock-induced electrical signals.

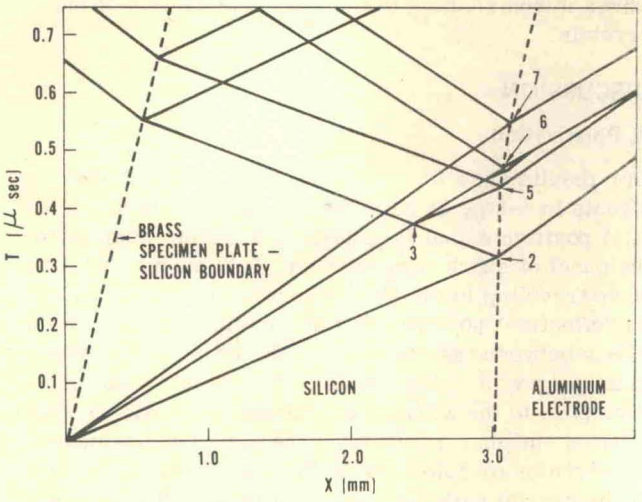

FIG. 2. x-t diagram of shock-wave propagation in silicon for the experimental arrangement of Fig. 1. The stresses behind the three forward-facing shock waves are 55, 133, and 162 kbar, respectively.

interpretation appears inconsistent with events noticed on our electrical records.

ELECTRICAL RECORDS

Figure 3(a) shows the voltage-time profile for a dynamic electrical resistance measurement at the 162-kbar loading pressure. In Fig. 3(a) the plane stress pulse enters the crystal specimen ~0.1 μsec after the oscilloscope was triggered at the time designated (0). The first inflection in the voltage-time profile occurring at (1) is at a voltage of 0.75 V. The significance of this inflection will be discussed later. The following inflection noted at (2) signals the arrival of the first elastic shock of 55 kbar at the Si—Al-electrode interface. [The inflection noted at (3) and (4) also will be discussed below using Fig. 3(b).] The second elastic shock makes its exit at (5). The voltage decreases to a new value at (6) when the first plastic shock arrives at the electrode. Then at the time (7) a small inflection again occurs in the waveform. This inflection denotes the arrival of the second plastic shock wave at the electrode. At that time the relative resistance change is 0.17 in response to an average stress of ~162 kbar in the crystal. Figure 3(b) is a waveform of the polarization voltage induced in a crystal by the calibrated 162-kbar stress from system No. 6 of Table I. The characteristics of the signal profile are nearly identical to Fig. 3(a) except that no voltage was imposed on the crystal. However, a positive voltage was generated at the shock front simultaneous with its impact and entry into the crystal at the time (0). The initial inflection in voltage was 0.55 V at (1), but the induced signal had its maximum value, 1.35 V, when the first elastic shock wave had completed its transit of the crystal at (2). At (3) the front of a backward-facing relief wave, which was reflected from the Si—Al-electrode interface, interacts with the first plastic wave front as was shown in Fig. 2. The total polarization begins to decrease. This decrease however is interrupted at (4), because of an increasing positive signal due to the second elastic wave which advances from the plane of interaction ahead of the plastic wave. At the time (5) this second elastic wave has left the crystal and the induced voltage again immediately begins to decrease. Zero potential is not recorded immediately on the exit of the second elastic wave because of relaxation effects, mechanical effects, and electronics response time. However, a state of zero potential is regained by the time (6) when the first plastic shock wave reaches the electrode and only the second plastic shock wave is still in the crystal.

Figure 4 gives the waveform of polarization signals generated in Si crystals by input stresses below the HEL. Si has a high shock impedance and when explosive-induced shocks are used, it is difficult to avoid exceeding its HEL. Therefore, an elastic-plastic wave separation method was used to obtain elastic input stresses. The crystals were impacted by the 21-kbar elastic precursor followed by the 130-kbar plastic I wave in the triple shock structure[13] of a steel driver plate. The precursor wave provided polarization signals at 12 kbar, the measured input stress for the Si crystal in Fig. 4. Several features are noted here which differ

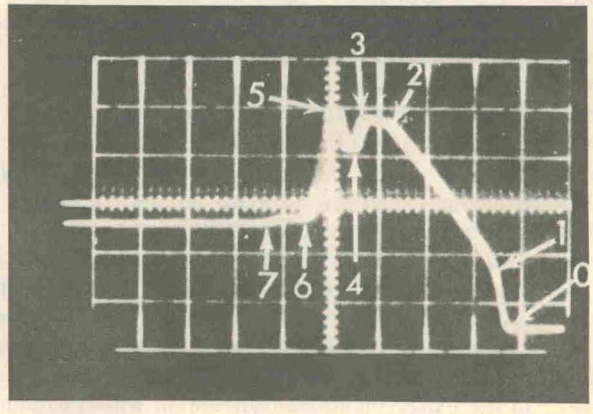

(a)

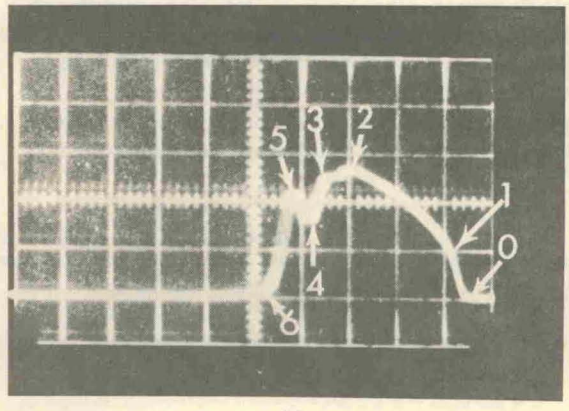

(b)

FIG. 3. (a) Oscilloscope record of a shock-wave resistance measurement of a silicon crystal. The crystal was stressed to 162 kbar. A voltage of −1.3 V was applied to the crystal. Time increases from right to left. The vertical scale is 0.5 V/div and the horizontal scale is 0.12 μsec/div. (b) Oscilloscope record of the induced positive voltage in a silicon crystal when stressed to 162 kbar. No voltage was applied to the crystal. Time increases from right to left. The vertical scale is 0.5 V/div and the horizontal scale is 0.12 μsec/div.

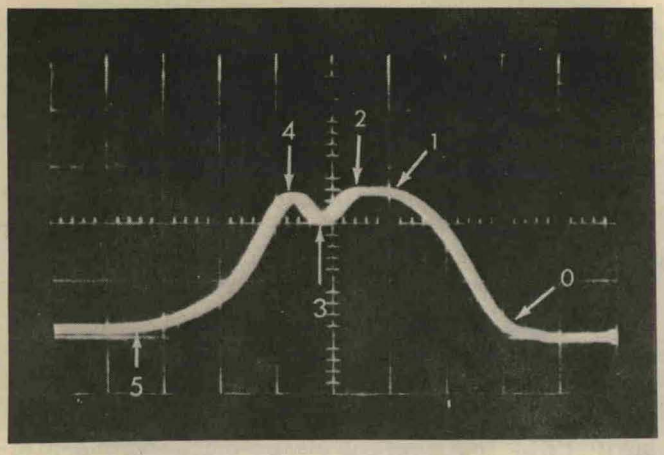

FIG. 4. Oscilloscope record of the induced positive voltage in a silicon crystal when stressed initially to 12 kbar. A second shock enters the crystal from the shock-driving system at ~0.4 μsec after the 12-kbar shock entered. This second shock takes the crystal to a stress of ~90 kbar. No voltage was applied to the crystal. Time increases from right to left. The vertical scale is 1.0 V/div and the horizontal scale is 0.11 μsec/div.

from the signal profile in Fig. 3(b). The waveform in Fig. 4 has no inflections prior to the arrival (2) of the 12-kbar elastic shock wave at the aluminum back-up electrode. The maximum signal (1) is 2.6 V as compared to 1.35 V in Fig. 3(b). After the 12-kbar wave leaves the crystal at (2) the signal amplitude begins to decrease until the time (3). A second elastic wave which enters near time (3) with a 33-kbar stress gradient (transmitted to the crystal by the 130-kbar plastic I shock in the steel driver) produces an increase again to the maximum polarization potential of 2.6 V at (4). The times at which the events (3) and (4) occur result from the separation in time, ~0.50 μsec between the elastic precursor front and the plastic I wave in the steel driver. In the experimental arrangement which produced Fig. 4, a number of elastic shocks reverberate between the steel-driver-plate—silicon interface and the oncoming plastic I shock in the steel. The effects of these reverberations should occur at times greater than ~0.4 μsec after the initial elastic shock enters the sample. Since few inflections occur in these electrical records, it is difficult to identify the roles of these waves in contributing to the total polarization of the crystals.

DISCUSSION

A. Polarization

Our results show that the shock-induced electrical signals in p-type Si have the following characteristics: (i) A positive signal is generated simultaneously with the onset of shock compression. This means that a shock wave traveling in the (111) direction in p-type Si carries an "effective" positive charge. (ii) An electric current exists between the end faces of the crystal only when an elastic wave is in the crystal. This result could imply, analogous to the acoustoelectric effect,[14] that the shock-induced emf may result from the simultaneous bunching of electrons or holes during the elastic wave's transit of the crystal with the majority carriers (holes in p-type Si) polarized by the wave in the direction of propagation. This effect of carrier dragging by the shock was proposed by Coleburn *et al.*[15] to explain the luminescence detected when a shock wave exits from chemically abraded aluminum oxide surfaces. More recently, similar luminescence and voltages produced during shock compression of europium[16] and other lanthanides were attributed to this effect. Harris[17] also offers a theoretical justification of shock-induced emf in semiconductors based on the acoustoelectric effect. (iii) For compressions in the plastic regime, an early inflection occurs in the induced emf signal. The inflection is labeled (1) in the electrical records, Figs. 3(a) and 3(b). Since it does not appear in the signal profile induced by shock compressions below the HEL, we speculate that it signals the onset of crystal yielding.[18] (iv) The maximum signal amplitude is obtained in response to stresses below the HEL. This result for p-type Si differs from the measurements of Graham *et al.*[19] who made resistivity measurements using n-type germanium with 10^{14} carrier concentration. They do not report polarization for elastic compressions.

Table II shows that the largest peak polarization signals are observed for stresses below the HEL, and that the peak amplitude of the signals decreases with increasing stress above the HEL. The peak polarization signal appears to be constant (2.6 V) for stresses below the HEL for initial temperatures of ~20 °C. The peak signal

TABLE II. Shock-induced electrical signals in p-type silicon (111).

System No.	Crystal[a] thickness (mm)	Initial resistance (Ω)	Stress amplitude[b] (kbar) First wave	Second wave	Third wave	Maximum signal (V)
1	3.50	9.0[c]	14			3.02
2	3.00	5.0	12			2.60
3	3.50	4.1	(8)			2.60
4	3.00	4.3	59			2.60
5	3.00	75.0	55	133		1.50
5	3.00	1300	55	133		1.48
6	3.02	4.4	55	133	162	1.35
7	3.02	4.1	55	133	(162)	1.20

[a] Crystal cross-sectional area 3.20 cm^2.

[b] Observed stress values behind the forward-facing shocks before wave interactions occur. Stresses are known to ± 10% except for values in parentheses which are known to ± 15%.

[c] Preheated sample at 139 °C (R_0 = 4.3 Ω at 20 °C). The other experiments were conducted at ~20 °C.

TABLE III. Relative resistance measurements.

System No.	Initial resistance, R_0 (Ω)	Stress[a] (kbar)	R/R_0[b]
2	4.00	(90)[c]	≤0.02
2	4.23	(90)	≤0.02
4	4.30	59	≤0.02
5	22.5	133	0.18
5	22.2	133	0.10
5	20.3	133	0.23
5	4.30	133	0.17
6	3.84	162	0.17
7	4.86	(162)	0.09

[a] Stress behind wave incident at Si-Al boundary at the time that the relative resistance measurement was made.
[b] The relative resistance was measured after the polarization had disappeared, e.g., near point (7) in Fig. 3(a). The smallest relative resistance measurable was 0.02.
[c] Stresses are known to ± 10% except for values in parentheses which are known to ± 15%.

increases to 3.02 V when a p-type Si single crystal is preheated to 139 °C, and then shocked elastically to 14 kbar. The peak polarization voltage for stresses above the HEL is not appreciably affected by the sample's initial resistance as seen in Table II. Two crystals with initial resistances of 1300 and 75 Ω each gave peak signals of about 1.5 V. This result when compared to the other signals' values may be attributed to a decrease in the transient resistance at the Si-Al interface on the shock-wave arrival. The characteristics of these records were affected by the initial resistances of the crystals and relatively low voltages occurred until the elastic shock wave reached the electrode. Then the maximum signal resulted and was in the form of a spike for the 1300-Ω crystal.

Zel'dovich[20] has offered an explanation of the shock-induced polarization based on the propagation of the double layer. If we assume, similarly to Mineev *et al.*,[21] that the electrical signals are primarily a response of the charged impurity particle to shock compression, the thickness r of the double layer is

$$r=\rho\epsilon U/\eta. \tag{1}$$

When the crystal is stressed by the 12-kbar shock in Table II, the resistivity behind the shock front is $\rho \simeq 1.0\ \Omega\,\text{cm}$, which corresponds to the resolution capability for our measurements. With the compressibility $\eta=0.926$ and the shock velocity $U=0.96$ cm/μsec, the dielectric constant $\epsilon=1.03\times10^{-10}$ C/N cm², we obtain $r=1.1\times10^{-6}$ cm. The measured potential difference $V_{max}=2.6$ V is related to the surface charge density,

$$\sigma=\eta V_{max}/AUR_L, \tag{2}$$

where the load resistor, $R_L=50\ \Omega$, and A, the crystal cross-section area is 3.2 cm². We obtain $\sigma=7.4\times10^{-9}$ C/cm². This value of σ corresponds to 7×10^{15} electrons/cm³ of the double layer, as compared to 10^{14} boron atoms/cm³ in our crystal specimens. This order-of-magnitude calculation suggests that the polarization is related to the impurity concentration, since each boron atom in p-type Si contributes a "hole" for ionization and conduction[22] with the same amount of charge as an electron but with a positive sign.

The growth of the induced emf signal can be described by

$$V(t)\propto[1-\exp(-t/\tau)], \tag{3}$$

where $V(t)$ is the voltage as a function of time t and τ is the relaxation time. A general argument for the use of an exponential expression to describe the growth in signal can be made, since it is a fundamental result from theories of rate processes. Other arguments also justify use of Eq. (3) in explaining the growth of the polarization signal. For example, a shock polarization model for dielectrics is used by Allison[23] to describe a mechanical contribution to the signal. He proposes that the shock front initiates a mechanical disturbance of the molecular dipoles, thereby creating in each element of the dielectric a net dipole moment per unit volume which decays with a characteristic relaxation time. A more fundamental model[24] for the shock polarization of semiconductors has been proposed which is based on the shifting of the energy levels behind the shock front. The voltage drop due to conduction across the shock front would also be represented by Eq. (3) for this theory if the sample's resistivity is small.

The recent work of Mineev *et al.*[7] on the polarization of silicon under shock conditions shows records similar to our results above the HEL for similar doping concentrations. However, they were unable to explain the roles of elastic and plastic waves in the polarization of Si. Their records of polarization of Si in the elastic region of stress are quite different from ours for corresponding doping levels. The three major differences are (i) the small magnitude of their signals in the elastic region, (ii) the emf decays behind an initial peak value, and (iii) the signals go negative when the elastic wave reaches the electrode. We have no satisfactory explanation for these different results. However, it is evident that at least a mechanical property difference exists in silicon crystals available in the USA and USSR. For example, Pavlovskii finds a value of 40 kbar for the HEL (dynamic yield) of (111) Si while our value is ~55 kbar, in agreement with the value reported by Gust and Royce. Also the Russian's value for the velocity of the elastic shock precursor is 8500 m/sec as compared with the USA value of 9600 m/sec measured in (111) Si at the HEL.

Earlier work on shocked copper-germanium junctions[25] gave electrical signals which were attributed to a thermoelectric effect, and inflections occurring in the records were identified with multiple shock waves in germanium. A second inflection occurring soon after the elastic shock left the crystal was interpreted as a possible new phase transition in germanium. It was pointed out that this inflection occurred at the time a backward-facing elastic relief wave interacts with the forward-facing plastic shock front. The wave interaction was not believed to be the cause of the inflection. We find, however, that the association of the inflection with the interacting waves agrees with our interpretation of the observed inflections occurring in the polarization records of p-type Si.

B. Shock resistance

There are certain limitations in our shock-resistance data of Table III which should be noted. We cannot ascertain all changes that occurred in the crystal structure during passage of the shock waves and what effect these changes had on the final resistance values. The polarization effect, however, was eliminated since the final values were measured when the polarization voltage was zero, e.g., corresponding to the times denoted (7) in Fig. 3(a).

The measurements show that the resistance becomes very small ($R/R_0 < 0.02$) for stresses near the HEL, indicating that a metallic state is reached. The resistance then increases, and for a stress of 133 kbar the relative resistance is ~0.17. When the crystals are shocked by stresses above 133 kbar, two plastic shocks occur which make the identification of the resistivity associated with each particular shock impossible. The values of the relative resistance, however, are correct for stresses within ± 10% of the stresses given in Table III. A curious result mentioned earlier is that the resistivity behind the second plastic shock is slightly larger than the resistivity behind the first plastic wave. For example, it was noted in Fig. 3(a) that the small inflection in the record at (7) gives a higher relative resistance (0.17) than the value (0.12) which is measured at (6). Remember that the numbers (6) and (7) denote, respectively, the arrival times of the first and second plastic shock waves at the electrode.

We consider the large increase in the relative value, R/R_0, that occurs between 90 and 133 kbar as independent evidence of a transition. The transition occurs at ~133 kbar as measured by free-surface measurements as discussed earlier, and most likely is a polymorphic transition.

The surprise in the data is the low resistance at the elastic stress level. For example, at 59 kbar the relative resistance decreases by > 98%. The corresponding static resistance data for crystalline Si[2,3] show a transition from the semiconductor to a metallic state at stresses ranging from 110 to 200 kbar. The introduction of large shear stresses in the static experiments caused the change to the metallic state to occur at the lower stresses. In our experiments even greater shear forces are present and are very rapidly applied. Therefore, the transition occurs under dynamic compression at significantly lower stress levels and much shorter times, e.g., in the microsecond interval of elastic shock compression near the HEL. The lower dynamic stresses required for conversion to the metallic state are additional evidence that the transition is strongly shear-rate dependent. The resistance data also imply that it was incorrect for Pavlovskii[1] to interpret the discontinuity at ~100 kbar in his dynamic compressibility measurements as a transition to the metallic state.

SUMMARY

In review, the complex effects, e.g., multiple shock-wave structure and polarization, have complicated our experiments to determine the effect of pressure on the resistance of silicon under shock conditions. Despite these complications useful data were obtained. The electrical experiments have clarified the roles of the elastic and plastic waves in the shock polarization behavior of silicon and assisted in the interpretation of its complicated Hugoniot. The resistance measurements imply a transition to the metallic state near the HEL which is shear-rate dependent. The resistance data also imply a polymorphic transition near 133 kbar.

Areas of future work can be recommended. An elastic precursor is likely to be present in most semiconductors under shock compression, and its effect in polarization experiments could contribute to a better understanding of the mechanism of conduction. The effect of variations in the impurity concentration should be studied once an understanding of the cause of the polarization is clearly ascertained. More electrical measurements in the elastic regime are clearly required. Resistivity experiments with the faces of the electrodes parallel to the shock motion (attached to the edges of the crystal) would be free of the polarization signal and allow easier interpretation of the observed resistance changes.

---

*Supported by the Naval Ordnance Laboratory Independent Research Fund.

[1]M. N. Pavlovskii, Sov. Phys.-Solid State **9,** 2514 (1968).
[2]S. Minomura and H. G. Drickamer, J. Phys. Chem. Solids **23,** 451 (1962).
[3]R. H. Wentorf, Jr. and J. S. Kasper, Science **139,** 338 (1963).
[4]G. E. Hauver, J. Appl. Phys. **36,** 2113 (1965).
[5]G. E. Hauver, Fifth ONR Report No. DR-163, 1970, p. 313 (unpublished).
[6]J. Y. Wong, R. K. Linde, and R. M. White, J. Appl. Phys. **40,** 4137 (1969).
[7]V. N. Mineev, A. G. Ivanov, Yu. V. Lisitsyn, E. Z. Novitskii, and Yu. N. Tyunyaev, Sov. Phys.-JETP **32,** 592 (1971).
[8]H. D. Jones, J. W. Forbes, and N. L. Coleburn, Bull. Am. Phys. Soc. **116,** 53 (1971).
[9]T.P. Liddiard and B.E. Drimmer, Soc. Motion Pict. Telev. Eng. **70,** 106 (1961).
[10]N. L. Coleburn, J. Chem. Phys. **40,** 71 (1971).
[11]W. H. Gust and E. B. Royce, J. Appl. Phys. **42,** 1897 (1971).
[12]The events designated (1) and (4) in the electrical records are not due to wave arrivals or interactions as will be explained in the next section.
[13]D. Bancroft, E. L. Peterson, and S. Minshall, J. Appl. Phys. **27,** 291 (1956).
[14]R. H. Parmenter, Phys. Rev. **113,** 102 (1959).
[15]N. L. Coleburn, M. Solow, and R. C. Wiley, J. Appl. Phys. **36,** 507 (1965).
[16]V. N. Mineev, A. G. Ivanov, Yu. V. Lisitsyn, E. Z. Novitskii, and Yu. N. Tyunyaev, Sov. Phys.-JETP **34,** 131 (1972).
[17]P. Harris, Picatinny Arsenal Report No. SMUPA-TK-2018, 1971 (unpublished).
[18]The time required for yielding cannot be obtained from the electrical records because of instrument response time and shock-wave tilt.
[19]R. A. Graham, O. E. Jones, and J. R. Holland, J. Phys. Chem. Solids **27,** 1519 (1966).
[20]Ya. B. Zel'dovich, Sov. Phys.-JETP **26,** 159 (1968).
[21]V. N. Mineev, A. G. Ivanov, E. Z. Novitskii, Yu. N. Tyunaev, and Yu. V. Lisitysn, JETP Lett. **5,** 269 (1967).
[22]C. Kittel, *Introduction to Solid State Physics* (Wiley, New York, (1966), p. 311.
[23]F. E. Allison, J. Appl. Phys. **36,** 2111 (1965).
[24]D. J. Pastine (private communication).
[25]J. Jacquesson, J. P. Romain, M. Hallouin, and J. C. Desover, Fifth ONR Report No. DR-163, 1970, p. 285 (unpublished).